Inorganic Chemistry

Article

pubs.acs.org/IC

Testing the Concept of Hypervalency: Charge Density Analysis of K_2SO_4

Mette S. Schmøkel,[†] Simone Cenedese,[‡] Jacob Overgaard,[†] Mads R. V. Jørgensen,[†] Yu-Sheng Chen,[§] Carlo Gatti,*[,‡] Dietmar Stalke,*[,∥] and Bo B. Iversen*[,†]

[†]Center for Materials Crystallography, Department of Chemistry and iNANO, Aarhus University, Langelandsgade 140, DK-8000 Aarhus C., Denmark

[‡]Istituto di Scienze e Tecnologie Molecolari del CNR (CNR-ISTM) and Dipartimento di Chimica, Università di Milano, via Golgi 19, I-20133, Milano, Italy

[§]ChemMatCARS, University of Chicago, Advanced Photon Source, Argonne, Illinois 60439, United States

[∥]Institut für Anorganische Chemie, Georg-August-Universität Göttingen, Tammannstrasse 4, 37077 Göttingen

Supporting Information

ABSTRACT: One of the most basic concepts in chemical bonding theory is the octet rule, which was introduced by Lewis in 1916, but later challenged by Pauling to explain the bonding of third-row elements. In the third row, the central atom was assumed to exceed the octet by employing d orbitals in double bonding leading to hypervalency. Ever since, polyoxoanions such as SO_4^{2-}, PO_4^{3-}, and ClO_4^- have been paradigmatic examples for the concept of hypervalency in which the double bonds resonate among the oxygen atoms. Here, we examine S−O bonding by investigating the charge density of the sulfate group, SO_4^{2-}, within a crystalline environment based both on experimental and theoretical methods. K_2SO_4 is a high symmetry inorganic solid, where the crystals are strongly affected by extinction effects. Therefore, high quality, very low temperature single crystal X-ray diffraction data were collected using a small crystal (∼30 μm) and a high-energy (30 keV) synchrotron beam. The experimental charge density was determined by multipole modeling, whereas a theoretical density was obtained from periodic ab initio DFT calculations. The chemical bonding was jointly analyzed within the framework of the Quantum Theory of Atoms In Molecules only using quantities derived from an experimental observable (the charge density). The combined evidence suggests a bonding situation where the S−O interactions can be characterized as highly polarized, covalent bonds, with the "single bond" description significantly prevailing over the "double bond" picture. Thus, the study rules out the hypervalent description of the sulfur atom in the sulfate group.

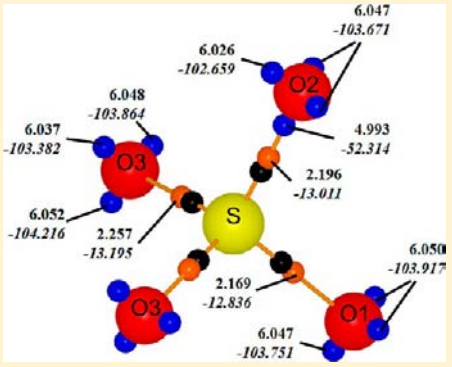

INTRODUCTION

The octet rule, as proposed by Lewis in 1916, is a cornerstone in chemistry.[1] It is one of the most important concepts, and the dash between two elements as a symbol for a two-electron-two-center-bond is the lowest common denominator in chemistry, spanning from preparative to theoretical chemistry. One of the oddities of this simple model is cases where the octet rule is violated because the central atom in a molecule has more than eight electrons in its valence shell. Such compounds are called *hypervalent*. The sulfate ion, SO_4^{2-}, is an archetypical example of an entity that is hypervalent according to the Lewis model, Figure 1. The hypervalency results from the introduction of double bonds in the structure leading to a count of 12 valence electrons for sulfur. The idea of double bonds, and thereby hypervalency, is supported by the short S−O bond lengths generally found from experiment and theory. An alternative description of the sulfate ion involves only single bonds and this avoids the issue of hypervalency (Figure 1). However, this description does not fulfill Pauling's electroneutrality requirement of minimizing the formal charges.[2] Pauling noted that the heavier atoms are not rigorously restricted by the octet rule, since they can make use of the d orbitals in bond formation.[3]

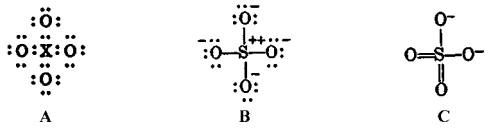

Figure 1. Polyoxoanion formula introduced by Lewis (A), the extreme sulfate structure, challenged by Pauling (B) and the representation with resonating double bonds, which he regarded as more satisfactorily (C).

The bonding situation in hypervalent molecules is still a topic of constant debate in theory[4] as well as in synthesis.[5] In the framework of the valence bond theory, the bonding in hypervalent molecules is described in terms of $d^n sp^3$ hybrid orbitals pursuant to the sp^n hybridization in molecules obeying

Received: June 27, 2012
Published: July 26, 2012

   dx.doi.org/10.1021/ic301372m | *Inorg. Chem.* 2012, 51, 8607−8616

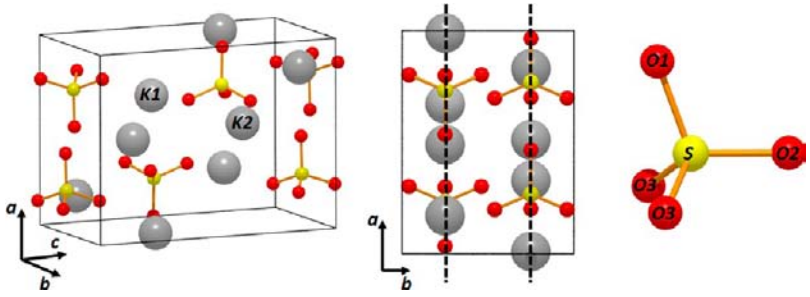

Figure 2. K_2SO_4 crystal structure. The unit cell is shown on the left. In the middle picture the unit cell is viewed along the *c* axis to highlight the trace (dotted line) of the σ planes (0 1/4 0) and (0 3/4 0). The sulfate group is shown on the right. Only the two non equivalent potassium (K1 and K2) atoms have been labeled in the left picture while the sulfur and all the oxygen atoms have been labeled in the right one to emphasize the mirror plane passing through S, O1 and O2.

the octet rule. However, calculations indicate that the necessary d orbitals in the optimization merely serve as polarization functions and do not contribute to the bonding by accommodating the additional valence electrons at the sulfur atom.[6] Nevertheless, this description is still found in various textbooks. An alternative description of the bonding in hypervalent molecules has been suggested by Rundle.[7] Already in 1947 he pointed out that in planar SO_x systems the formation of a π-electron system is feasible, which leads to an *m*-center-*n*-electron p_π-p_π-bonding, thus reducing the number of valence electrons around the central atom.

Today most of the theoretical approaches view the S−O bonding as polar single σ-bonds mainly characterized by electrostatic interactions.[6h−k] The general conclusion made by Cioslowski and Surján for the "hypervalent" molecules is that "*each of the formally double S−O bonds consists of one highly polarized covalent bond and one almost fully ionic bond*".[6h] This is a description where the octet rule is *not* violated. A similar view on the S−O bonding is given by Dobado et al. that characterize it as "*polar single σ-bonds mainly characterized by electrostatic interactions*".[8] Experimental studies have not been able to rule out hypervalency or precisely determine the bond order of S−O bonds.[8]

The hypervalent picture is expected to involve the presence of several resonance forms as opposed to the single bond case. At first sight, the number of lone pairs on the oxygen atoms differs in the two cases, Figure 1. This means that a characterization of the bonding and the number of lone-pairs in the sulfate group may give the information concerning which picture is more correct. However, both in the hypervalent and in the single-bonded situation all the oxygen atoms must reflect the occurrence (resonant or "static", respectively) of three lone pairs in their valence shell, and thus only the form and magnitude, rather than the number, of lone pair charge density concentrations should be affected. In charge density studies of hexacoordinated silicon,[9] iminophosphoranes,[10] and in the imine-analogues of SO_2 and SO_3, $S(NR)_2$, and $S(NR)_3$[11] the number of valence shell charge concentrations on the atoms was used to argue against hypervalency, but in the general case represented by the sulfate ion this is not conclusive evidence. According to the Quantum Theory of Atoms in Molecules (QTAIM)[12] another commonly used sign of double bond character, as revealed in terms of its π-electron features, is the so-called ellipticity of the bond. This is a measure of the deviation from a perfect cylindrical symmetry of the electron distribution around the bond, usually evaluated at the bond critical point. However, since the SO_4^{2-} group in a crystal has close to local T_d symmetry, the ellipticity value cannot significantly deviate from zero in this case, regardless of the single or double nature of the bond.

In the present paper we study the electron density of a sulfate-containing crystalline compound, K_2SO_4, which is chosen since it is highly ionic so that the actual charge of the sulfate group is close to the formal charge of −2 (Figure 2).

The aim of the study is to experimentally investigate the structure and electron density topology of K_2SO_4 and compare it with theoretical calculations. The hope is to contribute experimentally to the issues raised in various theoretical studies and to describe S−O bonding, which led to the concept of hypervalency, more resiliently. Even though K_2SO_4 is a simple compound, it presents a substantial challenge to experimental charge density determination because of the quite severe extinction observed for the low order reflections.[13] Accurate measurement of these reflections is important since they carry an important part of the valence electron information. Use of a high energy, high intensity synchrotron beam facilitates accurate diffraction experiments on micrometer sized crystals (∼30 μm) with much reduced absorption and extinction effects compared with conventional sources.[14]

EXPERIMENTAL SECTION

Data Collection. Single crystal synchrotron X-ray diffraction data were collected on a ∼20 × 30 × 30 μm^3 K_2SO_4 crystal at the ChemMatCARS beamline, 15-ID-B, at the Advanced Photon Source (APS), U.S.A. A Bruker APEXII CCD detector was used to record the diffracted intensities at λ = 0.41328 Å and T = 10(3) K. A total of six data runs were collected, each containing 1200 frames (a 360° φ-scan) except for run 4 and 6 with 590 and 600 frames, respectively. The two first runs contain low order data with the detector at 2θ = 10° and different ω-angles of 180° and 150°. The last four runs were collected with the detector at 2θ = 40° and ω-angles of 210°, 150°, 180°, and 150°, and these contain high order data up to sin θ/λ ∼ 1.34 $Å^{-1}$. The exposure time for the low order data was 0.5 s, while it was 2 s for the high order data. The second low order run was attenuated to avoid saturation of the detector.

Data Reduction. A more complete description of the data reduction can be found in the Supporting Information. The integration was carried out with *SAINT*+,[15] and the data were scaled in the program *SADABS*,[16] which was also used to carry out an absorption and oblique correction. For the latter correction the phosphor-absorption coefficient at a wavelength of 0.41328 Å is 0.6041. Finally, data averaging was performed with the program SORTAV.[17] Selected crystallographic data are listed in Table 1.

Multipole Refinements. The initial approach for the multipole refinement in the program XD2006[18] was to model the potassium atoms as ionic, spherical entities, K^+. For these refinements the SCM data bank in XD2006 were used since it contains data on ions. For sulfur, multipoles up to the hexadecapole level were refined while oxygen had

dx.doi.org/10.1021/ic301372m | *Inorg. Chem.* 2012, 51, 8607−8616

Table 1. Selected Crystallographic Information

formula	K_2SO_4
crystal system	orthorhombic
space group	*Pnma*
Z	4
formula weight (g/mol)	174.26
T (K)	10(3)
λ (Å)	0.41328
crystal size (μm)	~20 × 30 × 30
a (Å)	7.4053(2)
b (Å)	5.7080(2)
c (Å)	9.9768(3)
α, β, γ (°)	90
V (Å^3)	421.709(28)
completeness	99.2%
I_{meas}, N_{unique}	51598, 4402
R_{int}, $\langle N \rangle$	3.47%, 11.8
$(\sin\theta/\lambda)_{min}$, $(\sin\theta/\lambda)_{max}$ (Å^{-1})	0.084, 1.338

multipoles up to octupole level. In the refinements κ and κ' were constrained to be equal for both the sulfur and the oxygen atoms. Atomic positions and anisotropic Atomic Displacement Parameters (ADPs) were refined for all atoms. An isotropic type-1 extinction correction with a Lorentzian mosaic distribution was performed, and the data were also corrected for anomalous dispersion. Only reflections with $I > 3\sigma(I)$ and $\sin\theta/\lambda < 1.330$ Å^{-1} were included in the refinement. The resulting refinement residuals are listed in Table 2.

The results from this refinement are quite satisfactory taking into account the high resolution ($\sin\theta/\lambda$ up to 1.330 Å^{-1}), previous problems with extinction in refinement of conventional X-ray data from the same compound, and the fact that "heavy" elements are generally challenging to model in experimental charge density studies. However, when studying the scale factor variation across the resolution by plotting $\sum F_O^2/\sum F_C^2$ against $\sin\theta/\lambda$ relatively large deviation is observed for the low order data (Figure 3). Thus, the low-order reflections with $\sin\theta/\lambda <$ ~0.135 Å^{-1} (corresponding to the (101), (002), (011), (102), (111), and (200) reflections) are overestimated by the multipole model.

At first sight the deviation observed for the low order data could be caused by unmodeled extinction effects. However, an isotropic extinction correction was included in the model, and considering the crystal size and the high X-ray energy it seems unreasonable that this could have such a large impact. Indeed the largest extinction correction is 3.8% for reflection (020). Another explanation could be saturation of the detector for the intense low order reflections. For this reason a new set of low order data was collected together with a few runs of high order data. These data were collected on a slightly larger crystal (data not shown). In this data collection the low order data were measured both with and without strong attenuation to properly determine the intensities of the strongest reflections. However, the attenuated data set did not solve the problem of problematic scale factors in the low order data. The problem therefore appears to be related to insufficient modeling of the electron density. In the residual density some unmodeled density is observed around the potassium ions, Figure 4a. This could indicate that treating potassium as fully ionized with zero population of the 4s valence shell may not be entirely correct. If one examines the scattering factor for the diffuse 4s valence shell of potassium, it is seen that the main contribution to the scattering from the 4s orbital on K is found in the very low order region with $\sin\theta/\lambda <$ ~0.15 Å^{-1} (see Supporting Information). This is exactly the region causing problems in the plot of $\sum F_o^2/\sum F_c^2$.

To improve the modeling of the low order data a new model (Model 1) with neutral potassium atoms was tested (using the VM data bank in XD2006) and with the possibility for charge transfer through refinement of the monopole populations for all atoms. Because of the diffuseness of the 4s valence shells on the potassium atoms it was not possible to refine higher poles ($l > 0$) for this atom. In addition, another model, Model 2, was refined, identical to Model 1, but allowing κ and κ' on S and O, respectively, to vary freely instead of fixing them to be equal. The atomic positions and ADPs for Models 1 and 2 are tabulated in the Supporting Information together with multipole populations. The ADPs are identical for all models within the standard uncertainties and they are generally found to be higher than the values obtained in a 15 K structural study by Ojima et al.[13] Table 2 lists the refinement residuals, whereas Figure 4b shows the residual density obtained for Model 2. Figure 4 uses a cutoff of 0.9 Å^{-1} in the Fourier summation to better reveal possible unmodelled valence features. In the Supporting Information residual maps using the full data set are included, and these, as expected, contain more noise because of the weakness of the high order data.

The effect of treating the potassium atoms as either ionic or neutral is rather limited when considering the residual density, but a small improvement is seen for $R(F^2)$. When considering the scale factors there is a clear improvement for the low order data in the models with neutral potassium, Figure 2. The data point at lowest $\sin\theta/\lambda$ only contains one weak reflection (101). The major improvement with the model containing neutral potassium scattering factors is for the data bin with second lowest $\sin\theta/\lambda$. There are only small differences between Model 1 and Model 2 with the latter having slightly lower residuals. For both models, the static and dynamic deformation density maps show virtually identical features, Figure 5. This indicates that a proper deconvolution of thermal motion has been achieved. Given the similarities between the two models only Model 2, which is slightly more flexible, will be considered in the following discussion of the chemical bonding. Overall, it is quite remarkable to have diffraction data with an accuracy enabling explicit modeling of the very diffuse 4s electron on potassium.

Table 2. Refinement Residuals[a]

	K^+ model	model 1	model 2
N_{par}	96	98	98
N_{obs}	3298	3298	3298
$R(F)$, $R(F^2)$	0.0120, 0.0173	0.0114, 0.0155	0.0113, 0.0155
$lR_w(F^2)$, $R_{all}(F^2)$	0.0211, 0.0185	0.0194, 0.0167	0.0192, 0.0167
GOF	0.9668	0.8865	0.8815
max/min residuals	−0.416/+0.474	−0.440/+0.446	−0.436/+0.417
max ext. (013)	97.0%	98.3%	98.1%
max ext. (020)	96.2%	97.8%	97.6%
M(K1)	N/A	0.30(9)	0.44(10)
M(K2)	N/A	0.21(8)	0.17(9)
κ(S), κ'(S)	0.949(5)	0.943(4)	0.946(5), 0.86(2)
κ(O), κ'(O)	0.971(1)	0.983(2)	0.983(2), 1.21(7)

[a]Models 1 and 2 both use neutral potassium scattering factors and only differ in the number of radial kappa parameters. The K+ model uses an ionic scattering factor on potassium. See text for further details.

dx.doi.org/10.1021/ic301372m | Inorg. Chem. 2012, 51, 8607−8616

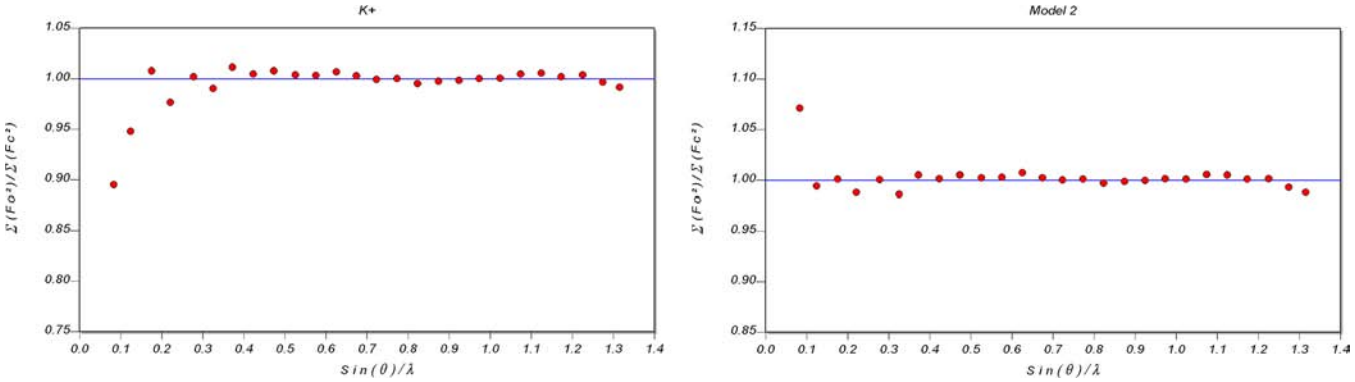

Figure 3. $\sum F_o^2/\sum F_c^2$ binned with respect to resolution shells and plotted against sin θ/λ from the multipole refinement using K^+ (top) and Model 2 (bottom).[29]

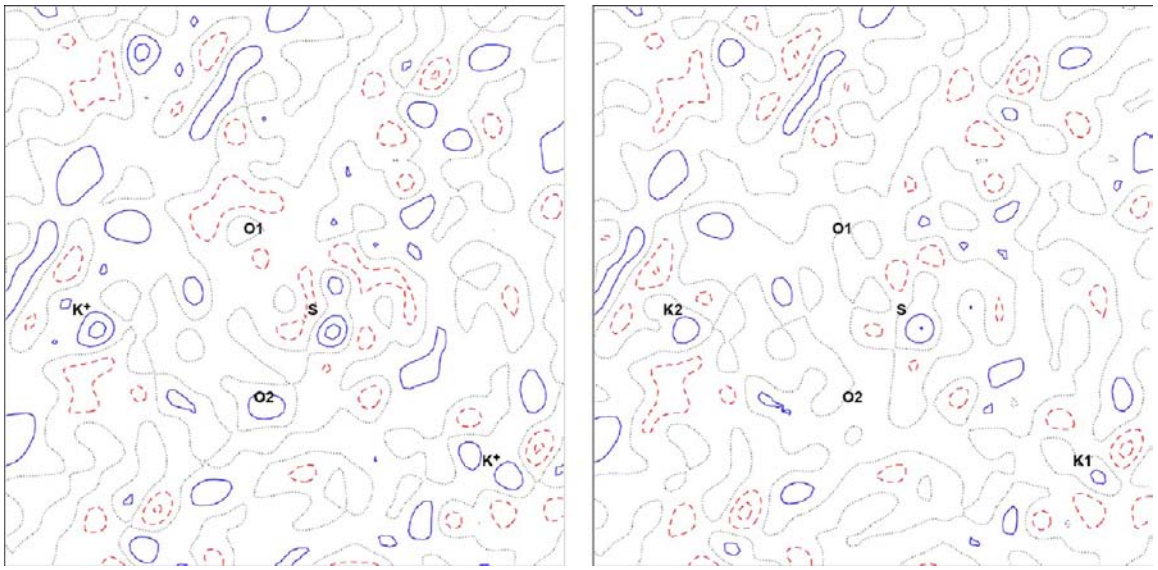

Figure 4. Residual density in the mirror plane for a model using a K^+ scattering factor (left) and with model 2 (right). Data with sin $\theta/\lambda < 0.9$ Å^{-1} were used in the Fourier summation. The contour interval is 0.1 e/Å^3. Positive contours are full, blue lines, while negative ones are dashed red lines. The zero contour is shown as black dotted lines.

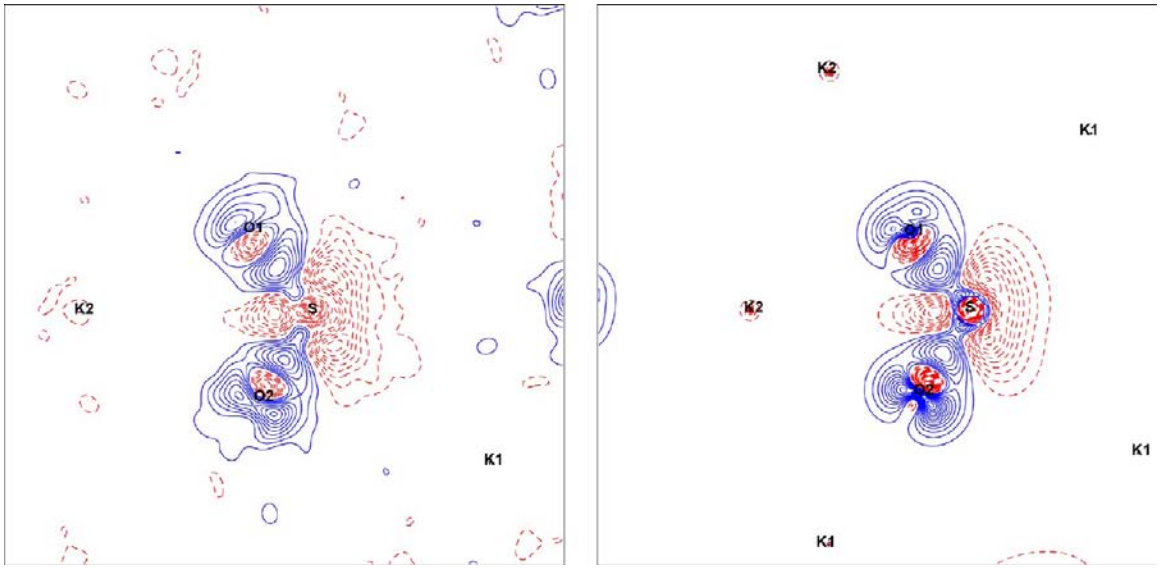

Figure 5. Dynamic (left) and static (right) model deformation density in the mirror plane obtained using Model 2. The contour interval is 0.05 e/Å^3. Positive contours are full, blue lines, while negative are dashed red lines.

dx.doi.org/10.1021/ic301372m | Inorg. Chem. 2012, 51, 8607−8616

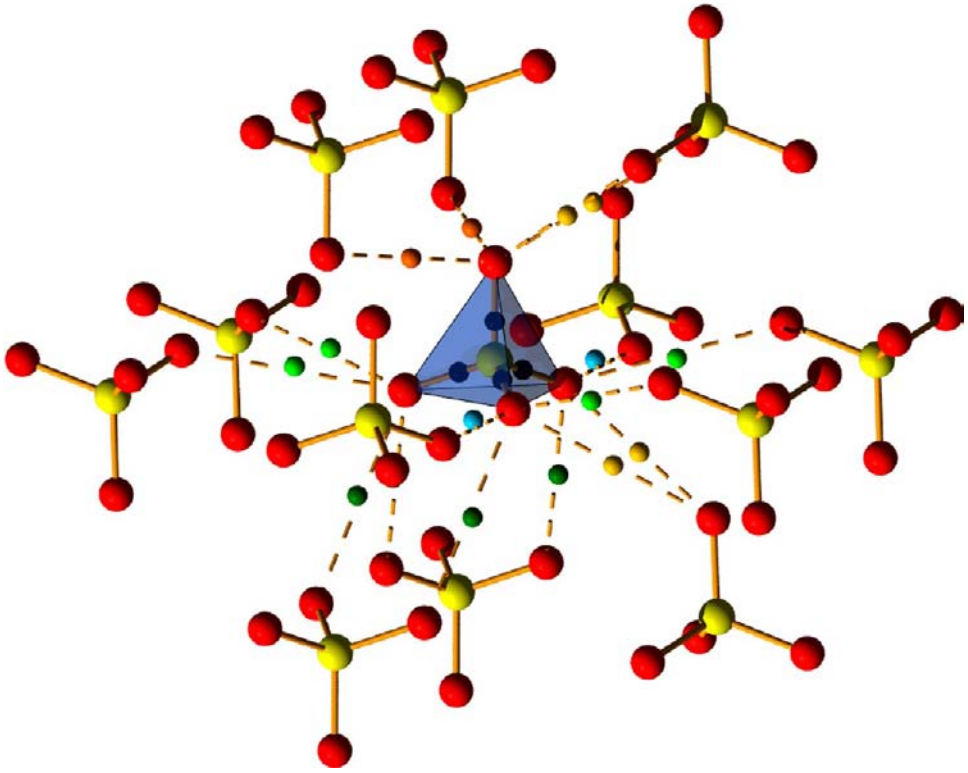

Figure 6. S−O and O−O bonding interactions within and among the sulfate groups as obtained from the theoretical electronic density. A tetrahedron is added to distinguish the central SO_4^{2-} from its 12 neighboring groups. Big yellow and red spheres represent S and O atoms respectively. The small colored spheres represent the oxygen−oxygen BCP position (see the Supporting Information), while the black ones mark those related to the S−O interactions.

Table 3. Topological Parameters for the Different Chemical Bonds Based on the Experimental (First Line) and Theoretical (Second Line) Charge Density[a]

		d (Å)	$AIL_{A\text{-}BCP}$ (Å)	$AIL_{BCP\text{-}B}$ (Å)	ρ (e/Å^3)	$\nabla^2\rho$ (e/Å^5)	ε
S−O1	exp	1.480	0.591	0.889	2.017	−0.213	0.014
	theo		0.590	0.891	1.943	10.221	0.004
S−O2	exp	1.467	0.588	0.879	2.038	1.280	0.018
	theo		0.585	0.882	1.988	12.355	0.004
S−O3	exp	1.477	0.591	0.885	2.031	1.107	0.076
	theo		0.588	0.889	1.957	10.817	0.004

[a] d is the bond distance between the two atoms. AIL (Å) is the length of the atomic interaction line, split in the contributions from the BCP to either one or the other bonded atom. ρ is the electron density (e/Å^3), $\nabla^2\rho$ the Laplacian (e/Å^5) and ε the ellipticity of the bond.

COMPUTATIONAL DETAILS

A theoretical electron density has been obtained from periodic ab initio density functional theory (DFT) calculations performed employing the program CRYSTAL06.[19] Basis sets of def2-TZVP quality[20] were used for the various atoms along with the B3LYP functional.[21] To avoid issues related to quasi-linear dependence of the basis set, the most diffuse s, p, and d Gaussian functions for the K atom were removed [ref 19, Chapter 7]. No modifications have been performed for the O and S basis set. The overall (s/p/d) contraction scheme therefore was: K (8421/631/11), S (73211/51111/21), O (62111/4111/11). The wave function was evaluated at the experimental geometry, but in addition two calculations were performed where (1) the atomic positions were optimized keeping cell edges fixed at the experimental values and (2) both atomic positions and lattice parameters were optimized while retaining the *Pnma* space group symmetry. No significant differences were found when evaluating electronic and topological properties from the three different periodic wave functions. In the following, only the results obtained from the wave function evaluated at the experimental geometry will be discussed.

RESULTS AND DISCUSSION

A complete topological analysis has been performed for both the experimental and the theoretical density.[12] For the experimental density the programs TOPXD and XDPROP from the XD2006 program package were used,[16] while TOPOND was employed for the theoretical density.[22] In general, the same overall picture is obtained from experiment and theory, although a few discrepancies can be found. The first general considerations concern the number of critical points (see Supporting Information for the full list). For the theoretical density the Morse relation $n - b + r - c = 0$ (n, b, r, and c being the number of attractors, bond (BCP), ring, and cage critical points, respectively) is fulfilled.[23] In the experimental electron density, a few critical points from the theoretical density are missing related to the longest (more than 3 Å) K2−O2 and O1−O3 interactions.[24] In general, for all the recovered K−O interactions and O−O interactions between the sulfate anions (Figure 6), the BCP is located far from the atomic valence shell charge

dx.doi.org/10.1021/ic301372m | *Inorg. Chem.* 2012, 51, 8607−8616

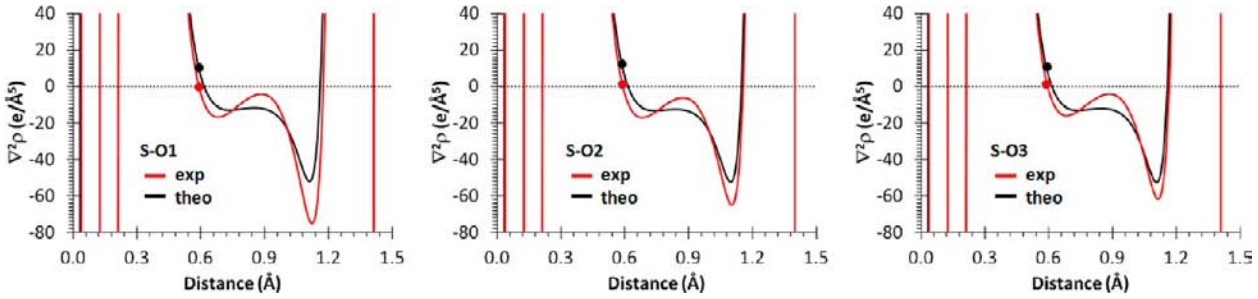

Figure 7. Laplacian profiles along the three S−O internuclear axes in the crystal for the theoretical (black line) and the experimental (red line) data. The black and red dots mark the position of the BCP. On the *x* axes the distance from the S atom is shown.

concentrations (VSCCs) and is characterized by a very low value of ρ, for both the experimental and the theoretical densities. This, combined with positive values of the Laplacian at the BCP (see Supporting Information) is an indication that these interactions have the expected ionic closed shell nature.

On the other hand, some differences between experiment and theory can be highlighted for the S−O interactions (Table 3 and Figure 7), which are the primary focus of the present paper. Considering the charge density obtained from experiment, the analysis of the sign of the Laplacian at the BCP would indicate a shared shell interaction for S−O1 and closed shell interactions for S−O2 and S−O3.[25] However, the absolute values of the Laplacian are rather small in all cases and do not assess the nature of the bonds when evaluated at the BCPs alone. The values obtained from theory are all clearly positive suggesting a closed-shell description. When studying the whole profile of the Laplacian along the internuclear axes for each of the three S−O bonds, and both for the experimental and theoretical densities, two local minima and a local maximum (i.e., a "double dip" in the $\nabla^2\rho$) are found in the region between the two bonded atoms. In a previous study such a feature has been taken as an indication of covalent character of the bonding.[61] The apparent discrepancies in the values obtained from experiment and theory can easily be rationalized when evaluating the behavior of $\nabla^2\rho$ around the BCP (Figure 7).

The S−O BCP is located in a rampant area of the Laplacian and even a small variation of the position of the BCP will change the Laplacian value drastically. If $|\nabla^2\rho|$ is not far from zero this also changes its sign. Considering this, the overall picture is that charge accumulation can be observed in the region between the sulfur and the oxygen atoms. Yet, because of the large charge transfer between them, this accumulation region fully belongs to the oxygen atom basin. This is seen in Figure 8, where a comparison is made between the Laplacian profiles for free and bonded atoms based on theoretical densities. The general shape of the sulfur and oxygen VSCCs can still be recognized in the molecule, but here the sulfur atomic VSCC falls entirely into the oxygen basin and prevails over the valence shell depletion of the free oxygen atom upon bond formation. This results in a large accumulation of charge in the bonding region with respect to the isolated atoms, but, in accordance with the different electronegativity of the S and O atoms, the major part of this charge is shifted toward the oxygen atom. The small negative or positive value found for the Laplacian at the BCP is simply due to the fact that this point lies close to, or even within, the region of charge depletion of the outermost core shell (*L* shell) of the sulfur atom.

In summary, even though small details differ, the overall picture of a shared-shell, but highly polarized S−O bond is evidenced from both experimental and theoretical densities. This

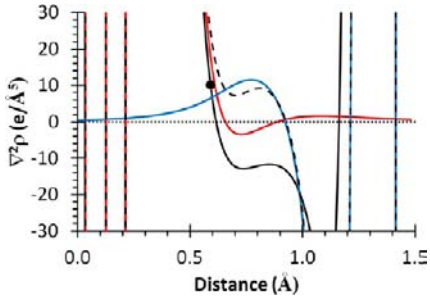

Figure 8. Laplacian profiles along the S−O1 internuclear axis in the crystal for the theoretical data. The profiles portrayed refer to the crystal (solid black) and to the isolated atoms (S: solid red; O: solid blue) Laplacian densities. The dashed black line represents the sum of the isolated atomic contributions. The discrepancy between this and the solid black line illustrates the reorganization of the atomic electron density upon bond formation. The black dot marks the position of the BCP in the crystal. On the *x* axis the distance from the origin, where the S atom is located, is shown.

description of the S−O bond is also supported by the two-dimensional contour plots and three-dimensional isosurfaces of the experimental Laplacian distribution shown in Figures 9 and 10.

From the contour plots in Figure 9, charge accumulation maxima can be seen within the VSCC of each oxygen atom. Although seen just in two dimensions (2D), it is tempting to identify these maxima with two oxygen lone-pairs and the S−O bonded charge concentration. From the 3D Laplacian surfaces in Figure 10 it is not easy to identify localized regions of charge accumulation for the oxygen atoms. Only for O3, and when using a contour level as high as −90 e/A^5, it is possible to discern three distinct accumulation regions. To more adequately identify VSCC maxima and their associated regions around the oxygen atoms, a topological analysis of $-\nabla^2\rho$ for its (3,−3) critical points has been performed. The resulting VSCCs are plotted, and the respective values given, in Figure 11 for the theoretical density. The experimental VSCCs values can be found in the Supporting Information.

The results reveal the presence of three maxima pointing away from the S−O bond for all oxygen atoms. These are usually indicated as *nonbonding maxima* (NBM) and are associated with lone pairs in Lewis theory. In addition to this, one (3,−3) maximum is found along each S−O bond, located in the O basin and close to the S−O BCP. These latter maxima, lying along the bond paths, are referred to as *bonding maxima* (BM). The presence of one BM and three NBMs for each oxygen atom accounts for their sp^3 hybridization and agrees well with the Lewis picture of a single and, because of the previously

dx.doi.org/10.1021/ic301372m | *Inorg. Chem.* 2012, 51, 8607−8616

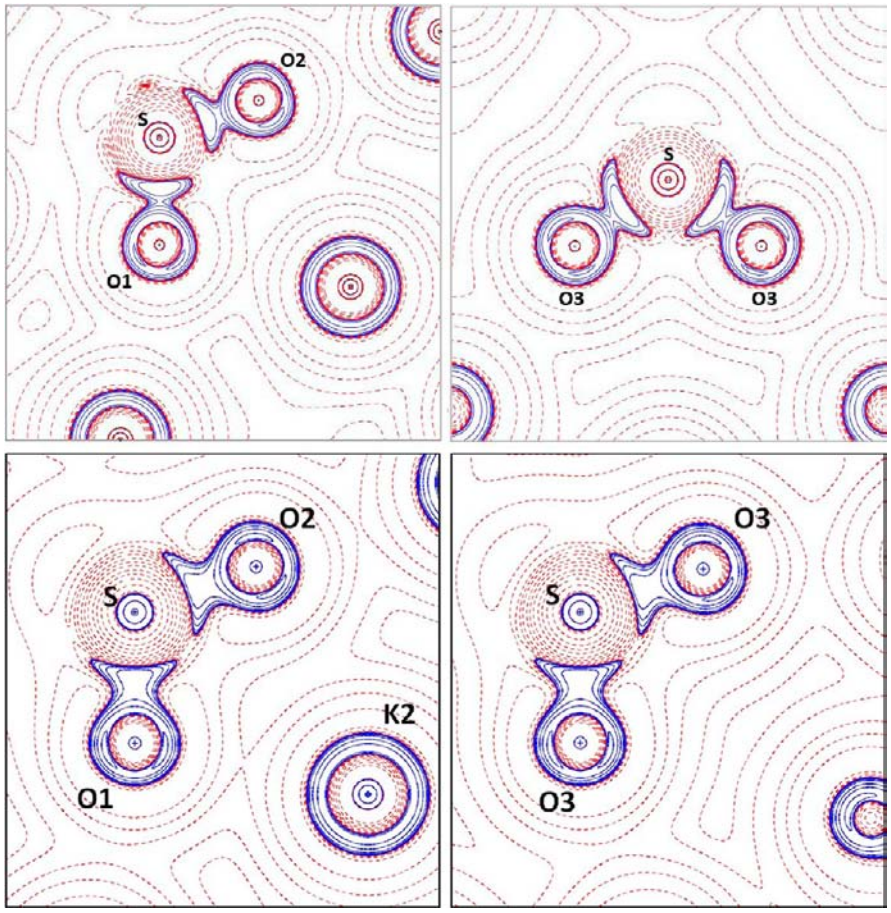

Figure 9. $\nabla^2\rho$ maps cut in the O1−S−O2 (left) and O3−S−O3 (right) plane of the crystal (top: experiment; bottom: theory). Solid blue lines mark regions of charge accumulation (negative $\nabla^2\rho$) while dotted red lines mark regions of charge depletion (positive $\nabla^2\rho$).

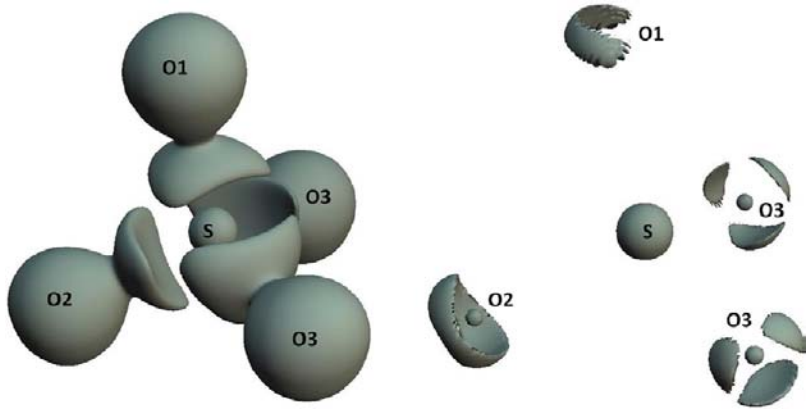

Figure 10. Three-dimensional plots of the Laplacian at contour levels of zero (left) and −90 e/Å^5 (right) for the experimental density.

mentioned BM location, polarized S−O bond. However, as anticipated in the introduction, three NBMs would also be compatible with the mixing of the various resonant forms corresponding to the purely hypervalent description (Figure 1). For the S−O2 interaction, an additional (3,−3) CP in the Laplacian is found close to O2 and along the S−O internuclear axis, see Figure 11. This fact is at first surprising since one would not expect to see a sign of decreased sharing for the shortest interaction, which is S−O2. However, it is rationalized considering that a bond length decrease unexpectedly leads to a more polarized S−O bond (see the source function and the delocalization indices analyses below). An almost identical global picture is obtained from the experimental data. The only noticeable differences are that also for O1 an additional (3,−3) CP in the Laplacian is found close to the oxygen and along the S−O internuclear axis, and that for O2 only two VSCC maxima pointing away from the sulfur atom are recovered (see Supporting Information, SI.5). At O2 the nonbonded VSCCs regions are strong but very broad in the experimental density, and, consequently, different maxima could not be assigned in the (3,−3) search. Inspection of Supporting Information, Figure S7 reveals that O2 exhibits the least departure from a spherical Laplacian distribution around the nucleus. The enhanced spherical character of the O2 basin could be the result of a

dx.doi.org/10.1021/ic301372m | *Inorg. Chem.* 2012, 51, 8607−8616

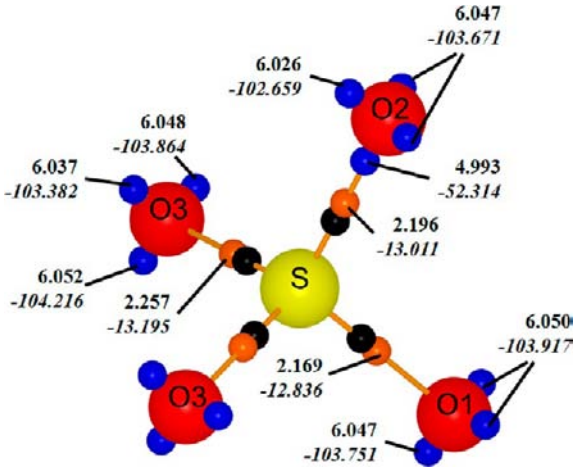

Figure 11. Bonded (BM) and nonbonded (NBM) maxima for the S−O interactions (theo). The small blue spheres represent the maxima found within the oxygen VSCCs and close to the oxygen nucleus (∼0.35 Å from the O nucleus) while the small orange spheres are the ones lying along the S−O bond paths, closer to the sulfur atom (∼0.74 Å from the S nucleus) but still located in the oxygen basins. The values of ρ and its Laplacian (italic) are given for each maximum. The small black spheres mark the position of the BCPs.

greater weight of the resonant form with a "double bond" for the S−O2 interaction (which is the shortest one). Indeed, as shown later in this paper, shortening the S−O bond leads to a decrease in the charge concentration of the O lone pairs and to increased spherical character of the O density. As a consequence, location of maxima in the VSCC shell may become numerically problematic in this case and be the cause of the missing third NBM on O2, a situation which is not encountered with the theoretical density.

Table 4 lists QTAIM atomic charges obtained from atomic basin integrations of all unique atoms both for the experimental and the theoretical data. As expected the net charges of the potassium atoms are close to +1*e*. The experimentally obtained QTAIM net atomic charge on each of the four oxygen atoms is on average around −1.4*e* and the net charge on sulfur is around +4.3*e* giving an overall charge of −1.36*e* for the sulfate anion. The theoretical QTAIM charges are very similar. Thus, the net charge on S is only slightly lower (+3.9*e*), and the potassium net charges are slightly higher (∼0.9*e*, compared with ∼0.75*e* from experiment). Cioslowski and Surján interpret their large QTAIM atomic charges in SO-containing compounds as proof of a large degree of ionicity in the bonds.[6h]

Table 4. QTAIM Atomic Charges Obtained from the Experimental (exp) and the Theoretical (theo) Electron Density

		K1	K2	S	O1	O2	O3
Q	exp	0.72	0.77	4.27	−1.37	−1.39	−1.43
	theo	0.90	0.90	3.86	−1.42	−1.41	−1.42

As a further characterization of the bonding features in K_2SO_4, a Source Function (SF) analysis has been performed.[26] Table 5 lists the percentage contribution, %SF(Ω), from the various atomic basins to the electron density at the S−O BCPs based on the theoretical density. Corresponding values from the experimental density are listed in the Supporting Information. About 79% of the density at the BCP is determined by the sulfur and its linked oxygen atom. This value is comparable to that found for prototypical nonpolar covalent bonds such as the C−C single bond in ethane[26b] and indicates that the valence charge involved in bonding is localized, but not as much as found in conventional covalent double bonds (%SF around 85−90%).

Table 5. %SF Contributions to S−O BCPs Theoretical Electron Densities[a]

bond	S	O1	O2	O3	$O3_\sigma$	TOT
S−O1	28.5	49.4	6.8	6.7	6.7	98.2
S−O2	29.5	6.4	50.0	6.5	6.5	98.9
S−O3	28.6	6.6	6.8	49.6	6.6	98.3
$S-O3_\sigma$	28.6	6.6	6.8	6.6	49.6	98.3

[a]The symbol $O3_\sigma$ identify the oxygen atom equivalent to O3 due to the presence of the mirror plane.

The large difference between the %SF values of the bonded S and O atoms at their BCP clearly confirms the very polarized nature of the S−O shared bond. It is furthermore important to note the non-negligible %SF contribution from the other O atoms to each S−O BCP (Table 5). The cumulative effect from these atoms amounts to ∼20% of each S−O BCP density, which is around 2/3 of the density determined at the same point by the sulfur atom. This looks like an unexpected result for a single-bond depiction of the S−O bond in the sulfate ion (Figure 1), and one could naively be tempted to simply ascribe it to the proximity of the oxygen atoms and the inverse dependence of the distance to the reference point in the local source function expression.[26] However, the importance of the neighboring oxygen atoms for the S−O bonding in the sulfate group is neatly corroborated by the large electron exchange existing between the oxygen atoms which is reflected in the values of the delocalization indices $\delta(O,O')$.[27] Table 6 reports %SF and $\delta(O,O')$ values calculated for a T_d molecular model of the sulfate group evaluated at the equilibrium S−O distance as well as for elongated and shortened S−O bonds.

Before discussing the data in Table 6, recall that the number of electrons $N(\Omega)$ in an atomic basin, Ω, is the sum of those that are fully localized within the basin, $\lambda(\Omega)$, and half of those that are delocalized (exchanged) between Ω and the remaining basins (second term in the right-hand expression of eq 1).

$$N(\Omega) = \lambda(\Omega) + \frac{1}{2}\sum_{\Omega' \neq \Omega} \delta(\Omega', \Omega) \quad (1)$$

For typical nonpolar single, double, and triple covalent bonds, like the C−C bond in ethane, ethene, and acetylene, the values of $\delta(C,C')$ are almost equal to 1, 2, and 3, respectively. When a bond is largely polarized, electrons are less effectively exchanged and, as an example, the value of $\delta(C,O)$ for the C═O molecule is only about 1.6−1.8 . Considering the S−O bond at the equilibrium distance, $\delta(S,O)$ is 0.92 indicating that S and O are exchanging about one electron as expected for a covalent single bond or for a highly polarized single bond with partial double bond character. The number of electrons delocalized between each pair of oxygen atoms, $\delta(O,O')$ = 0.22, is not negligible. In fact, the sum of electrons each oxygen exchanges with the neighboring oxygen atoms in the sulfate anion is only 20−30% less than the electrons it exchanges with the sulfur atom to which it is directly bonded. When the S−O bond is forced to shorten or elongate, the contribution of the various resonant forms to the hypothetical hypervalent bonding scheme (Figure 1c) is expected to increase or decrease, respectively. Thus, in a hypervalent bonding description an enhanced degree of "double-

dx.doi.org/10.1021/ic301372m | Inorg. Chem. 2012, 51, 8607−8616

Table 6. %SF Contributions for the S−O BCP in a T_d Model for the Sulfate Group at Equilibrium (Bold), Shortened and Elongated Bond Distance[a]

d (Å)	ρ (e/Å^3)	%SF(S)	%SF(O)	$\sum_O$%SF(O′)	δ(S,O)	$\sum_O\delta$(O,O′)	Q (O)	NBM (e/Å^5)
1.4250	2.130	26.4	51.4	21.8	0.81	0.74	−1.53	99.8
1.4650	1.993	28.0	50.6	21.2	0.86	0.71	−1.48	102.6
1.5050	**1.872**	**29.8**	**49.6**	**20.3**	**0.92**	**0.67**	**−1.42**	**105.4**
1.5450	1.764	32.1	48.4	19.1	0.98	0.63	−1.35	108.2
1.5850	1.665	34.8	47.1	17.7	1.06	0.59	−1.27	111.0

[a]Delocalization indices δ, the net oxygen charge Q(O), and the value of the negative of the Laplacian density at one of the three equivalent oxygen lone pair concentrations, NBM, are also reported for the various S−O distances.

bond" character is expected upon shortening of the S−O bond. This picture is supported by the increase in the density at the BCP and by the trend in the δ(O,O′) and %SF values indicating an increasing capability of the oxygen atoms to exchange electrons with each other with decreasing S−O distance. The increased availability of electrons in the bonding region with decreasing S−O distance is paralleled by a decrease in the charge concentration of the lone pairs as seen from the NBMs $-\nabla^2\rho$ values. However, unexpectedly the electron exchange between S and O (and thus the bond order) diminishes with decreasing S−O distance, and the source function contribution from the S and O atoms to the BCP density decreases. The δ(S,O) value diminishes from 1.06 at an S−O distance d = 1.5850 Å to 0.81 at d = 1.4250 Å, while the sum of %SF contributions from the oxygen and the sulfur atoms show a parallel decrease from 81.9 to 77.9%. The decrease of δ(S,O) and the %SF(S+O) contribution is accompanied by a clear increase of the bond polarity. Thus, the ratio %SF(S)/%SF(O) lowers from 0.74 at d = 1.5850 Å to only 0.51 at d = 1.4250 Å. Note that a homopolar bond would have a ratio of 1 at any distance. In other words, the SF not only mirrors the changes in the electron density exchange described by the delocalization indices, but also provides a rationale for such changes. The unexpected decrease in electron delocalization observed with decreasing distance is the result of a strongly enhanced bond polarization. This is seen in the large increase in charge transfer observed with decreasing distance as reflected in the Q(O) values in Table 6.

Overall, when forcing the S−O bonds to be shorter, that is, when increasing the imagined hypervalent bonding, the opposite picture of what would be expected from a conventional hypervalent bonding picture is observed. For shortened S−O bonds the bond order decreases rather than increases because of a counterbalancing effect arising from the large enhancement of the bond polarity. The electronic charge transferred from the lone pair regions to the S−O bonding region when decreasing the S−O bond distance turns out to be essentially localized on the oxygen basins.[28] This explains why the oxygen atoms increase their ability to exchange electrons among themselves upon S−O shortening, despite the fact that the electron exchange with the sulfur atom is decreased. Such a complex behavior, though ruling out any hypervalent description of the S atom, suggests a partial contribution to bonding in the sulfate ion from resonant forms that have a so polarized character that the actual S−O bond order at equilibrium does not exceed that of a standard covalent single bond.

CONCLUSIONS

The electron density of K_2SO_4 has been evaluated from multipole modeling of experimental synchrotron X-ray diffraction data and periodic DFT calculations. An excellent model with limited extinction effects was obtained from the multipole refinement of the experimental data. This is to the best of our knowledge the first experimental study of a sulfate anion in a crystalline environment, which includes a comprehensive topological analysis and characterization of the S−O bonding. The topology of the experimental and theoretical electron density show some minor differences, but are in overall good agreement and the same chemical picture is obtained. The S−O interactions can be characterized as highly polarized, covalent bonds, with the "single bond" description discharging the "double bond" picture.

Source Function (SF) analysis provided additional insights on the bonding description *dilemma* in K_2SO_4. The SF quantified the different extent to which the S and O bonded atoms determine the density at the BCPs, hence giving a measure of bond polarity and deviation from covalency. It also revealed a significant contribution from the neighboring oxygen atoms to the S−O bonding. When the S−O distance is decreased, the S−O bond unexpectedly becomes less covalent and even more polar. At the same time the neighboring oxygen atom involvement increases, and electronic charge is transferred from the oxygen lone pairs to the S−O bonding region. However, this charge is kept very close to the oxygen nucleus and not shared with sulfur atom. The bonding picture was corroborated by analysis of the delocalization indices. When the S−O bonds are shortened relative to equilibrium, the lone pair electrons on the other oxygen atoms are forced to participate in the bonding formally enhancing the S−O "double bond" character. However, at the same time the electron sharing between S and O decreases since the charge transfer between these atoms concomitantly increases.

Overall, a picture emerges in which there is a partial contribution to bonding in the sulfate ion from resonant forms enabling a significant electron exchange among the oxygen atoms. However, the S−O bond has such a polarized character that the actual S−O bond order does not exceed that of a standard covalent single bond. The present bonding analysis therefore rules out the hypervalent description of the S atom.

ASSOCIATED CONTENT

Supporting Information

Additional information on the data reduction and the multipole refinement including lists of refined parameters, full list of bond critical points (BCPs), Laplacian profiles for K−O and O−O interactions, topological analysis of the Laplacian of the experimental electron density, and source function analysis of the experimental electron density. This material is available free of charge via the Internet at http://pubs.acs.org.

dx.doi.org/10.1021/ic301372m | Inorg. Chem. 2012, 51, 8607−8616

AUTHOR INFORMATION

Corresponding Author

*E-mail: carlo.gatti@istm.cnr.it (C.G.), dstalke@chemie.uni-goettingen.de (D.S.), bo@chem.au.dk (B.B.I.).

Notes

The authors declare no competing financial interest.

ACKNOWLEDGMENTS

This work was supported by the Danish National Research Foundation (Center for Materials Crystallography), the Danish Strategic Research Council (Center for Energy Materials), the Danish Research Council for Nature and Universe (Danscatt), the Deutsche Forschungsgemeinschaft (Priority Program 1178), and the CaSuS Doctoral Program of the Land Niedersachsen. ChemMatCARS Sector 15 is principally supported by the National Science Foundation/Department of Energy under Grant NSF/CHE-0822838. Use of the Advanced Photon Source was supported by the U.S. Department of Energy, Office of Science, Office of Basic Energy Sciences, under Contract No. DE-AC02-06CH11357.

REFERENCES

(1) Lewis, G. N. *J. Am. Chem. Soc.* **1916**, *38*, 762−785.

(2) Pauling, L. *J. Chem. Soc.* **1948**, 1461−1467.

(3) Pauling, L. *The nature of the chemical bond*; Cornell University Press: Ithaca, NY, 1939.

(4) (a) Gillespie, R. J.; Silvi, B. *Coord. Chem. Rev.* **2002**, *233*−*234*, 53. (b) Noury, S.; Silvi, B. *Inorg. Chem.* **2002**, *41*, 2164.

(5) (a) Akiba, K. Y. *Heteroat. Chem.* **2011**, *22*, 207. (b) Ochiai, M.; Miyamoto, K.; Hayashi, S.; Nakanishi, W. *Chem. Commun.* **2010**, *46*, 511.

(6) (a) Mezey, P. G.; Haas, E. C. *J. Chem. Phys.* **1982**, *77*, 870−876. (b) Kutzelnigg, W. *Angew. Chem., Int. Ed. Engl.* **1984**, *23*, 272. (c) Cruickshank, D. W. J.; Eisenstein, M. *J. Mol. Struct.* **1985**, *130*, 143. (d) Cruickshank, D. W. J. *J. Mol. Struct.* **1985**, *130*, 177. (e) Mayer, I. *J. Mol. Struct. THEOCHEM* **1987**, *149*, 81. (f) Yu, W.; Guo, L. W.; Lin, H. C.; Kao, C. T.; Tsai, C. J.; Bats, J. W. *Inorg. Chem.* **1988**, *27*, 520−523. (g) Reed, A. E.; Schleyer, P. v. R. *J. Am. Chem. Soc.* **1990**, *112*, 1434. (h) Cioslowski, J.; Surján, P. R. *J. Mol. Struct. THEOCHEM* **1992**, *87*, 9. (i) Cioslowski, J.; Mixon, S. T. *Inorg. Chem.* **1993**, *32*, 3209. (j) Dobado, J. A.; Martínez-García, H.; Molina, J. M.; Sundberg, M. R. *J. Am. Chem. Soc.* **1998**, *120*, 8461. (k) Stefan, T.; Janoschek, R. *J. Mol. Model.* **2000**, *6*, 282. (l) Love, I. *J. Phys. Chem. A* **2009**, *113*, 2640−2646.

(7) Rundle, R. E. *J. Am. Chem. Soc.* **1947**, *69*, 1327.

(8) (a) Bats, J. W.; Coppens, P.; Koetzle, T. F. *Acta Crystallogr., Sect. B* **1977**, *33*, 37−45. (b) Wang, Y.; Chang, N. L.; Pai, C. T. *Inorg. Chem.* **1990**, *29*, 3256. (c) Figgis, B. N.; Khor, L.; Kucharski, E. S.; Reynolds, P. A. *Acta Crystallogr., Sect. B* **1992**, *48*, 144−151. (d) Figgis, B. N.; Iversen, B. B.; Larsen, F. K.; Reynolds, P. A. *Acta Crystallogr., Sect. B* **1993**, *49*, 794−806. (e) Lee, C. R.; Tang, T. H.; Chen, L.; Wang, Y. *Chem.—Eur. J.* **2003**, *9*, 3112−3121.

(9) Kocher, N.; Henn, J.; Gostevskii, B.; Kost, D.; Kalikhman, I.; Engels, B.; Stalke, D. *J. Am. Chem. Soc.* **2004**, *126*, 5563.

(10) Kocher, N.; Leusser, D.; Murso, A.; Stalke, D. *Chem.—Eur. J.* **2004**, *10*, 3622.

(11) (a) Leusser, D.; Walfort, B.; Stalke, D. *Angew. Chem., Int. Ed.* **2002**, *41*, 2079. (b) Leusser, D.; Henn, J.; Kocher, N.; Engels, B.; Stalke, D. *J. Am. Chem. Soc.* **2004**, *126*, 1781. (c) Henn, J.; Leusser, D.; Ilge, D.; Stalke, D.; Engels, B. *J. Phys. Chem. A* **2004**, *108*, 9442. (d) Stalke, D. *Chem.—Eur. J.* **2011**, *17*, 9264−9278. (e) Stalke, D. *Chem. Commun.* **2012**, 10.1039/c2cc33221c

(12) Bader, R. F. W. *Atoms in molecules. A quantum theory*; Oxford University Press: Oxford, U.K., 1990.

(13) Ojima, K.; Nishihata, Y.; Sawada, A. *Acta Crystallogr., Sect. B* **1995**, *51*, 287−293.

(14) (a) Clausen, H. F.; Overgaard, J.; Chen, Y. S.; Iversen, B. B. *J. Am. Chem. Soc.* **2008**, *64*, 7988−7996. (b) Poulsen, R. D.; Bentien, A.; Chevalier, M.; Iversen, B. B. *J. Am. Chem. Soc.* **2005**, *127*, 9156−9166. (c) Macchi, P.; Larsen, F. K.; Schultz, A.; Iversen, B. B. *J. Phys. Chem. A* **2001**, *105*, 9231−9242. (d) Overgaard, J.; Schiøtt, B.; Larsen, F. K.; Schultz, A. J.; Macdonald, J. C.; Iversen, B. B. *Angew. Chem., Int. Ed.* **1999**, *38*, 1239−1242. (e) Iversen, B. B.; Larsen, F. K.; Pinkerton, A.; Martin, A.; Darovsky, A.; Reynolds, P. A. *Acta Crystallogr., Sect. B* **1999**, *55*, 363−374.

(15) *SAINT*; Bruker AXS Inc.: Madison, WI, 2007.

(16) Sheldrick, G. M. *SADABS*; University of Göttingen: Göttingen, Germany, 1997.

(17) Blessing, R. H. *J. Appl. Crystallogr.* **1997**, *30*, 421−426.

(18) Volkov, A.; Macchi, P.; Farrugia, L. J.; Gatti, C.; Mallinson, P.; Richter, T.; Koritsanszky, T. *XD2006 - A Computer Program Package for Multipole Refinement, Topological Analysis of Charge Densities and Evaluation of Intermolecular Energies from Experimental and Theoretical Structure Factors*; 2006

(19) Dovesi, R.; Saunders, V. R.; Roetti, C.; Orlando, R.; Zicovich-Wilson, C. M.; Pascale, F.; Civalleri, B.; Doll, K.; Harrison, N. M.; Bush, I. J.; D'Arco, Ph.; Llunell, M. *CRYSTAL06*, User's Manual; University of Torino: Torino, Italy, 2006.

(20) Weigend, F.; Ahlrichs, R. *Phys. Chem. Chem. Phys.* **2005**, *7*, 3297−3305.

(21) (a) Becke, A. D. *J. Chem. Phys.* **1993**, *98*, 5648−5652. (b) Lee, C.; Yang, W.; Parr, R. G. *Phys. Rev. B* **1988**, *37*, 785−789.

(22) Gatti, C. *TOPOND98: an electron density topological program for systems periodic in N (N=0−3) dimensions, User's Manual*; CNR-ISTM: Milano, Italy, 1999; a new version interfaced to *CRYSTAL06* was used, also able to perform the calculation of the atomic source function contributions.

(23) Morse, M.; Cairns, S. S. *Point theory in global analysis and differential topology; an introduction*; Pure and applied mathematics a series of monographs and textbooks; Academic Press: New York, 1969.

(24) The electron density, ρ, and its Laplacian, $\nabla^2\rho$, are very flat in the regions of these interactions and the mentioned critical points could be missing in the experimental density just because of numerical inaccuracy of the BCP search procedure in *XD2006*.

(25) Bader, R. F. W.; Essen, H. *J. Chem. Phys.* **1984**, *80*, 1943−1960.

(26) (a) Bader, R. F. W.; Gatti, C. *Chem. Phys. Lett.* **1998**, *287*, 233. (b) Gatti, C.; Lasi, D. *Faraday Discuss.* **2007**, *135*, 55. (c) Farrugia, L. J.; Macchi, P. *J. Phys. Chem. A* **2009**, *113*, 10058−10067. (d) Gatti, C. *Struct. Bonding (Berlin)* **2012**, *147* 193286. (e) Lo Presti, L.; Gatti, C. *Chem. Phys. Lett.* **2009**, *476*, 308−316.

(27) Fradera, X.; Austen, M. A.; Bader, R. F. W. *J. Phys. Chem. A* **1999**, *103*, 304−314.

(28) This observation, and the unexpected decrease of electron sharing between S and O when decreasing their bond distance, explains why the single bonded maximum in S-O1 and S-O3 splits, for the shortest S-O2 bond, into two bonded maxima, one of which lies very close to the oxygen. It also explains why the lone pair NBMs on O2 have a smaller value than those on O1 and O3 (Figure 11).

(29) The plots are made with program XDRKplot which is implemented in the WinGX program package: Farrugia, L. J. *J. Appl. Crystallogr.* **1999**, *32*, 837.